

1 Macaque-human differences in SARS-CoV-2 Spike antibody response elicited by vaccination or
2 infection

3

4 Short title: Macaque vs. human antibodies to SARS-CoV-2 Spike

5

6 Alexandra C. Willcox,^{1,2,3} Kevin Sung,⁴ Meghan E. Garrett,^{1,3} Jared G. Galloway,⁴ Megan A.

7 O'Connor,^{5,6} Jesse H. Erasmus,^{5,7} Jennifer K. Logue,⁸ David W. Hawman,⁹ Helen Y. Chu,⁸ Kim J.

8 Hasenkrug,¹⁰ Deborah H. Fuller,^{5,6,11} Frederick A. Matsen IV,⁴ Julie Overbaugh^{1*}

9

10 ¹ Human Biology Division, Fred Hutchinson Cancer Research Center, Seattle, WA, USA

11 ² Medical Scientist Training Program, University of Washington, Seattle, WA, USA

12 ³ Molecular and Cellular Biology Program, University of Washington, Seattle, WA, USA

13 ⁴ Public Health Sciences Division, Fred Hutchinson Cancer Research Center, Seattle, WA, USA

14 ⁵ Department of Microbiology, University of Washington, Seattle, WA, USA

15 ⁶ Infectious Diseases and Translational Medicine, Washington National Primate Research

16 Center, Seattle, WA, USA

17 ⁷ HDT Bio, Seattle, WA, USA

18 ⁸ Department of Medicine, University of Washington, Seattle, WA, USA

19 ⁹ Laboratory of Virology, Division of Intramural Research, National Institute of Allergy and

20 Infectious Diseases, National Institutes of Health, Hamilton, MT, USA

21 ¹⁰ Laboratory of Persistent Viral Diseases, Division of Intramural Research, National Institute of

22 Allergy and Infectious Diseases, National Institutes of Health, Hamilton, MT, USA

23 ¹¹ Center for Innate Immunity and Immune Disease, University of Washington, Seattle, WA, USA

24

25 * Corresponding author

26 Email: joverbau@fredhutch.org

27 **Abstract**

28 Macaques are a commonly used model for studying immunity to human viruses, including for
29 studies of SARS-CoV-2 infection and vaccination. However, it is unknown whether macaque
30 antibody responses recapitulate, and thus appropriately model, the response in humans. To
31 answer this question, we employed a phage-based deep mutational scanning approach (Phage-
32 DMS) to compare which linear epitopes are targeted on the SARS-CoV-2 Spike protein in
33 humans and macaques following either vaccination or infection. We also used Phage-DMS to
34 determine antibody escape pathways within each epitope, enabling a granular comparison of
35 antibody binding specificities at the locus level. Overall, we identified some common epitope
36 targets in both macaques and humans, including in the fusion peptide (FP) and stem helix-
37 heptad repeat 2 (SH-H) regions. Differences between groups included a response to epitopes in
38 the N-terminal domain (NTD) and C-terminal domain (CTD) in vaccinated humans but not
39 vaccinated macaques, as well as recognition of a CTD epitope and epitopes flanking the FP in
40 convalescent macaques but not convalescent humans. There was also considerable variability in
41 the escape pathways among individuals within each group. Sera from convalescent macaques
42 showed the least variability in escape overall and converged on a common response with
43 vaccinated humans in the SH-H epitope region, suggesting highly similar antibodies were
44 elicited. Collectively, these findings suggest that the antibody response to SARS-CoV-2 in
45 macaques shares many features with humans, but with substantial differences in the
46 recognition of certain epitopes and considerable individual variability in antibody escape
47 profiles, suggesting a diverse repertoire of antibodies that can respond to major epitopes in
48 both humans and macaques.

49 **Author summary**

50 Non-human primates, including macaques, are considered the best animal model for studying
51 infectious diseases that infect humans. Vaccine candidates for SARS-CoV-2 are first tested in
52 macaques to assess immune responses prior to advancing to human trials, and macaques are
53 also used to model the human immune response to SARS-CoV-2 infection. However, there may
54 be differences in how macaque and human antibodies recognize the SARS-CoV-2 entry protein,
55 Spike. Here we characterized the locations on Spike that are recognized by antibodies from
56 vaccinated or infected macaques and humans. We also made mutations to the viral sequence
57 and assessed how these affected antibody binding, enabling a comparison of antibody binding
58 requirements between macaques and humans at a very precise level. We found that macaques
59 and humans share some responses, but also recognize distinct regions of Spike. We also found
60 that in general, antibodies from different individuals had unique responses to viral mutations,
61 regardless of species. These results will yield a better understanding of how macaque data can
62 be used to inform human immunity to SARS-CoV-2.

63 Introduction

64 The COVID-19 pandemic has created a pressing need to understand immunity to SARS-CoV-2,
65 both in the setting of vaccination and infection. This has prompted numerous studies in non-
66 human primates (NHPs), which are considered the most relevant animal model for studying
67 many infectious diseases of humans. Various NHP models have been employed to study the
68 immunogenicity and protective efficacy of SARS-CoV-2 vaccine candidates, with most studies
69 using macaque species including rhesus macaques (*Macaca mulatta*) [1-23], cynomolgus
70 macaques (*Macaca fascicularis*) [8, 24-32], and pigtail macaques (*Macaca nemestrina*) [22, 33-
71 35]. Some of these models have also been used to study infection and re-infection [35-39]. In
72 the NHP model, studies typically measure virus neutralizing antibody responses to vaccination
73 or infection. However, no study has investigated the fine binding specificities of both
74 neutralizing and non-neutralizing SARS-CoV-2 antibodies in macaques and how they compare to
75 the human responses they are meant to model.

76 Coronaviruses such as SARS-CoV-2 enter host cells using their Spike glycoprotein, which is
77 composed of trimeric S1 and S2 subunits. Receptor-binding S1 homotrimers protrude out from
78 the surface of the virion like a crown, giving this family of viruses its name, while the fusion-
79 mediating S2 trimers anchor the protein to the viral membrane. On S1, the receptor-binding
80 domain (RBD) of SARS-CoV-2 Spike protein binds to angiotensin-converting enzyme 2 (ACE2) on
81 host cells [40, 41]. For subsequent membrane fusion to occur, the Spike protein must be
82 cleaved by host cell proteases at the S1/S2 boundary and at an S2' site located just upstream of
83 the fusion peptide (FP) of S2 [42], leading to substantial conformational changes that likely
84 unmask new epitopes of S2 to immune cells [43].

85 Antibodies to SARS-CoV-2 Spike protein are especially interesting as a potential correlate of
86 protection, as they have the capacity to block infection and kill infected cells [44-47]. There has
87 understandably been great interest in studying neutralizing antibodies against the RBD, given
88 that such antibodies can directly block interaction with host cells. While RBD-directed
89 antibodies indeed contribute disproportionately to neutralization [48], the majority of the anti-
90 Spike plasma IgG response in convalescent individuals is directed to epitopes outside of the
91 RBD [49, 50]. RBD-directed antibodies are also less likely to maintain activity against future viral
92 strains, given the increasing number of variants of concern that harbor mutations in the RBD
93 and have reduced sensitivity to neutralization by immune plasma [51]. Additionally, growing
94 evidence from studies in humans and animal models indicates that non-neutralizing antibodies
95 play a role in protection [52-57].

96 Previous studies have used Phage-DMS [58], a tool that combines phage display of linear
97 epitopes with deep mutational scanning, to interrogate the fine binding specificities and escape
98 profiles of binding antibodies against all domains of Spike in infected and vaccinated humans
99 [59, 60]. These studies have shown that infection-induced human polyclonal antibodies
100 consistently bind linear epitopes in the FP and stem helix-heptad repeat 2 (SH-H) epitope
101 regions, with patient-to-patient variability in escape profiles [59]. Comparatively, mRNA
102 vaccination induces a broader antibody response across Spike protein with more consistent
103 escape profiles [60].

104 In this study, we built on this foundation by using Phage-DMS to study the binding and escape
105 profiles of antibodies in vaccinated and convalescent macaques in comparison to humans. Our
106 data reveal broad overlap in some major epitopes targeted by both macaques and humans,

107 though neither vaccinated nor convalescent macaques perfectly model the human response.
108 We also find considerable variability in individuals' antibody escape pathways in most epitope
109 regions in both macaques and humans. The broadest responses were seen in vaccinated
110 humans and re-infected rhesus macaques, groups that also share more concordant escape
111 profiles. These results have implications for the interpretation of COVID-19 macaque research
112 studies.

113 **Results**

114 Four groups were included in this study: vaccinated pigtail macaques, vaccinated humans,
115 convalescent (re-infected) rhesus macaques, and convalescent humans (Table 1). The
116 vaccinated macaques received a replicating mRNA (repRNA) vaccine encoding the full-length
117 wildtype (not pre-fusion stabilized) SARS-CoV-2 A.1 lineage Spike protein formulated with a
118 cationic nanocarrier [35, 61]. The vaccine was delivered as a prime-only 25ug (n=3) or 250ug
119 (n=6) dose or prime-boost 50ug dose (n=2), with plasma collected 42 days after the first dose
120 (n=9) or 14 days after the second dose (n=2). The vaccinated humans received two doses of the
121 100ug Moderna mRNA-1273 vaccine encoding the pre-fusion stabilized full-length SARS-CoV-2
122 A.1 lineage Spike protein and formulated with a lipid nanoparticle. Serum was collected from
123 human vaccinees 36 days after the first dose (7 days after the second dose). The convalescent
124 macaques were infected twice with SARS-CoV-2, with infections spaced six weeks apart and
125 serum collected 56 days after the first infection (14 days after the second infection). The
126 convalescent humans were naturally infected once with SARS-CoV-2 and exhibited mild disease,
127 with a median of 67 days between symptom onset and sample collection. Details of individual
128 participants are available in Table S1.

129 **Table 1.** Details of samples used in the current study.

Group	Number of samples	Age range (years)	Treatment	Time of sample collection
Vaccinated pigtail macaques	11	3 ½ - 6	repRNA vaccine encoding full-length SARS-CoV-2 Spike ^a	42 days post 1 st dose
Vaccinated humans	15	18 - 55	100ug mRNA vaccine encoding full-length pre-fusion stabilized SARS-CoV-2 Spike (Moderna)	36 days post 1 st dose
Convalescent rhesus macaques	12	2 ½ - 5	Infected twice with SARS-CoV-2 six weeks apart ^a	56 days post 1 st infection
Convalescent humans	12	28 - 52	Naturally infected once with SARS-CoV-2 (mild disease)	Median 67 (IQR 62, 70) days post symptom onset

130 ^aWithin each group of macaques, subgroups received slightly different treatments (described in Table S1).

131 **Enrichment of wildtype peptides**

132 To compare which regions of Spike protein are recognized by human and macaque antibodies,
133 we examined the enrichment of wildtype peptides by antibodies from each individual (Fig 1A).

134 Broadly speaking, binding was observed in the NTD, CTD, FP, and stem helix-HR2 epitope
135 regions as reported previously in human studies [59, 60]. Epitope regions (shown as different
136 colors on Fig 1) were defined as previously [60]: NTD, amino acid 285-305; FP, 805-835; stem
137 helix-HR2 (SH-H), 1135-1170. For the CTD, the bounds of epitope regions were expanded and
138 altered from previous studies based on macaque antibodies recognizing a wider area than
139 previously seen in humans: CTD-N', 526-593; CTD-C', 594-685 (S1A Fig). Several additional
140 epitopes that flank previously-defined regions were also identified in this analysis: pre-FP, 777-
141 804; post-FP, 836-855 (S1B Fig); and HR2, 1171-1204 (S1C Fig). Specific epitope regions can be

142 visualized on the structure of a Spike protein monomer in Fig 1B. In addition to these defined
143 regions, we noted that one convalescent rhesus macaque appeared to weakly recognize an
144 epitope at the beginning of the S2 subunit (amino acid 686-710, Fig 1A).

145 In general, we did not detect responses in the RBD because many epitopes in this region are
146 known to be conformational, and Phage-DMS only has the power to detect epitopes that
147 include linear sequences. Epitopes in the RBD have been extensively detailed elsewhere [62,
148 63]. However, we did detect strong binding to an RBD epitope in some vaccinated pigtail
149 macaques (Fig 1A). This same region was enriched in samples from before vaccination in four of
150 the five pigtail macaques with baseline samples available (S2 Fig). Pre-infection serum from the
151 twelve rhesus macaques did not show any consistent responses (S2 Fig). Because the RBD
152 response in pigtail macaques was present prior to vaccination with SARS-CoV-2 Spike, we did
153 not investigate it further as a response to vaccination.

154 To quantify differences in the epitopes targeted by different groups, the enrichment of wildtype
155 peptides was summed across each epitope region for every individual. Because the main
156 research question is whether responses in macaques model those in humans, two comparisons
157 were performed: vaccinated macaques vs. vaccinated humans and convalescent macaques vs.
158 convalescent humans (Fig 2).

159 In concordance with a qualitative assessment of the enrichment heatmap in Fig 1A, vaccinated
160 humans preferentially recognized the following epitope regions compared to vaccinated
161 macaques: NTD (Mann-Whitney $p \leq 0.01$), CTD-C' ($p \leq 0.0001$), and FP ($p \leq 0.05$) (Fig 2A).
162 Meanwhile, convalescent macaques recognized the following epitope regions more than
163 convalescent humans: CTD-N' ($p \leq 0.01$), pre-FP ($p \leq 0.001$), and post-FP ($p \leq 0.01$) (Fig 2B). All

164 groups consistently recognized the SH-H epitope region (Fig 2). While vaccination appeared to
165 induce a stronger response against HR2 than infection (Fig 1A), there were no significant
166 differences in response driven by species (Fig 2). Within each group of macaques (vaccinated
167 and convalescent), subgroups received slightly different treatments (Table S1), so similar
168 analyses were performed comparing these subgroups; no comparisons were significant at a
169 threshold of $p=0.05$ (Kruskal-Wallis test, S3 Fig).

170 Taken together, these findings indicate: 1) vaccinated humans were the only group to
171 consistently recognize peptides from both the NTD and CTD-C' epitope regions, which are in
172 close physical proximity to one another (Fig 1B); 2) convalescent humans had a limited
173 response to the CTD-N'; 3) compared to other groups, convalescent macaques had a notably
174 more robust response to regions upstream and downstream of the main FP epitope region; 4)
175 vaccinated macaques did not recognize the FP as strongly as other groups; and 5) vaccination
176 seemed to induce a stronger response against HR2 than infection in both macaques and
177 humans.

178 **Defining and comparing escape pathways**

179 To assess differences in the binding characteristics of human and macaque antibodies on a
180 more granular level, we next examined the mutations in Spike that reduced antibody binding in
181 each epitope region of interest. Because the antibody escape pathways for vaccinated humans
182 have been described previously [60], we did not examine the NTD and CTD-C', which are
183 exclusively recognized by this group. Instead, we focused on comparing escape profiles
184 between groups in the following epitope regions: CTD-N', FP, and SH-H. We first represent the
185 data as scaled differential selection values in logo plot form, as commonly shown in previous

186 studies. Importantly, scaled differential selection is highly correlated with peptide binding as
187 measured by competition ELISA [58]. To summarize the data represented by the logo plots by
188 group, summed differential selection values across each epitope region were also calculated.
189 This metric represents the overall magnitude of escape at each locus regardless of the specific
190 amino acid substitution, with negative values indicating a decrease in binding compared to the
191 wildtype amino acid, and positive values indicating enhanced binding (see “Materials and
192 Methods”). Finally, escape similarity scores were calculated between pairs of individuals to
193 quantify similarity in escape profiles (see “Materials and Methods” and S4 Fig).

194 **CTD-N’**

195 Vaccinated macaques, vaccinated humans, and convalescent macaques recognized peptides in
196 the CTD-N’ (AA 526-593), whereas convalescent humans generally did not (Fig 2B). Within this
197 epitope region, the individual escape profiles showed notable variability both within and
198 between groups (S5 Fig). For example, across all groups, some individuals showed relatively
199 high sensitivity to mutations between sites 558-567, while others had a response focused more
200 downstream around AA 577-586. There was also substantial variability in which loci in the CTD-
201 N’ had the highest relative magnitude of escape, and sometimes even in the directionality of
202 scaled differential selection at a given locus. For example, some individuals had antibodies that
203 bound mutated peptides better than wildtype at AA 555 (e.g., convalescent macaque 353)
204 while others exhibited reduced binding to mutated peptides (e.g., convalescent macaque 358).
205 The same was true for site 560 (e.g., vaccinated humans M24 and M26 exhibited improved and
206 disrupted binding to mutated peptides, respectively).

207 To summarize the trends observed in the individual findings, we calculated summed differential
208 selection values for each individual at each site and generated boxplots by group (Fig 3A). In
209 addition to the aforementioned regions of escape common to all groups, convalescent
210 macaques also showed considerable escape between AA 529-535, with vaccinated macaques
211 also showing a less consistent response in this area (Figs. 3A and S5). The complexity and
212 variability of the escape pathways also prompted us to quantify the similarity in escape
213 between and within groups. Escape similarity scores largely corresponded to areas of high
214 magnitude of escape. Sites with low-magnitude summed differential selection values indicate
215 loci where mutations have no notable impact, and therefore those escape profiles reflect
216 fluctuations in peptide enrichments due to noise, which drives a lower escape similarity score
217 at those sites (Fig 3A, lower panel). At some sites (e.g., 560, as described above), low scores
218 were also the result of some samples showing negative differential selection and others
219 showing positive differential selection, a comparison that was assigned the highest cost in our
220 escape similarity score algorithm.

221 To test the similarity of escape profiles across the CTD-N' epitope region, escape similarity
222 scores were aggregated across the region and computed both within and between groups.
223 These are shown as boxplots, with each point representing a pairwise comparison between
224 individual samples (Fig 3B). For example, every vaccinated macaque was compared to every
225 other vaccinated macaque (a within-group comparison) and to every vaccinated human (a
226 between-group comparison). We included a comparison of convalescent macaques and
227 vaccinated humans, given visual similarities between their patterns of escape (Fig 3A).
228 Convalescent macaques showed the highest within-group similarity in escape profiles, meaning

229 their escape profiles were more consistent than those of the vaccinated macaques or
230 vaccinated humans (Fig 3B). Between-group escape similarity scores were on par with the
231 within-group scores for the vaccinated macaques and humans, indicating that although there
232 was substantial variability in individual profiles, this was not driven by sample groups.

233 **FP**

234 Escape profiles were examined in the FP epitope region (AA 805-835) for the three groups that
235 showed significant wildtype enrichment in this area: vaccinated humans, convalescent
236 macaques, and convalescent humans. As in the CTD-N', overall there was variability in
237 individual escape profiles, though the convalescent macaques showed a more consistent
238 pattern of escape than other groups (S6 Fig). Within the FP, most sites of escape fell between
239 AA 811-825 for all groups (Fig 4A). The convalescent macaques again exhibited the highest
240 escape similarity scores (Fig 4B). The median within-group escape similarity scores in the FP
241 were on par with those in the CTD-N' (Fig 3B), indicating approximately equal variability in
242 antibody escape in these epitope regions. The between-group escape similarity scores were
243 generally similar to each other and to the human within-group scores (Fig 4B).

244 **SH-H**

245 All four groups consistently recognized peptides spanning the SH-H epitope region (AA 1135-
246 1170). Major sites of escape were located between AA 1145-1158 for all groups (Fig 5A). The
247 individual logo plots in the SH-H suggested a consistent response among vaccinated humans
248 and convalescent macaques, with more variability in the remaining groups (S7 Fig). This finding
249 is supported by the within-group escape similarity scores for those groups trending higher
250 across the epitope region (Figs. 5A lower panel and 5B). The median epitope region-wide

251 escape similarity scores for vaccinated humans and convalescent macaques were also higher in
252 the SH-H than in the CTD-N' or FP, confirming a more concordant response. The median
253 between-group escape similarity score for vaccinated humans and convalescent macaques was
254 on par with their median within-group scores, indicating that the escape profile of a vaccinated
255 human looks as similar to that of a convalescent macaque as it does to another vaccinated
256 human (Fig 5B). The similarity between these two groups was higher than the similarity
257 between convalescent macaques and humans, as well as between vaccinated macaques and
258 humans (Fig 5B). Despite this overall trend, two vaccinated humans had more unique escape
259 profiles (S7 Fig, M26 and M19) and are responsible for a cluster of lower-similarity outlier
260 points (Fig 5B, "Vaccinated Humans" and "Conv. Mac. vs. Vacc. Hum.").

261 The pairwise comparison between participant 352 (a convalescent macaque) and M21 (a
262 vaccinated human) generated an escape similarity score closest to the median for all
263 comparisons between these groups. Logo plots for these individuals are shown in Fig 5C as a
264 representative example of the striking between-group similarity. The most consistent sites of
265 escape for both groups were AAs 1148, 1152, 1155, and 1156 (Figs. 5A and S7). While some
266 differences exist, there was not nearly as much variability as in the CTD-N' (S5 Fig) and FP (S6
267 Fig).

268 **Other epitope regions**

269 In addition to the epitope regions described above, the convalescent macaques strongly
270 recognized the pre-FP and post-FP, which were not targeted by human antibody responses (S8
271 Fig). Escape profiles in the pre-FP appeared highly consistent among individual macaques, with
272 major sites of escape at AAs 795, 798, 800, and 802. Profiles were more variable in the post-FP,

273 likely due in part to low enrichment of wildtype peptides in this epitope region for some
274 individuals (S8 Fig).

275 **Comparison of vaccinated humans and convalescent macaques**

276 It was notable that the vaccinated humans and convalescent macaques showed the most
277 similarity in escape profiles across all epitope regions, most strikingly in the SH-H. Thus, we also
278 asked whether they showed similarity in the epitopes they targeted by comparing the
279 enrichment of wildtype peptides in these groups in each epitope region (S9 Fig). Vaccinated
280 humans recognized the following epitope regions more strongly than convalescent macaques:
281 NTD (Mann-Whitney $p \leq 0.0001$), CTD-C' ($p \leq 0.0001$), and HR2 ($p \leq 0.001$). Convalescent
282 macaques preferentially recognized the pre-FP ($p \leq 0.0001$) and post-FP ($p \leq 0.001$) epitope
283 regions. This suggests some diversity in the epitopes targeted, but similarity of antibody escape
284 patterns within epitopes targeted by both groups.

285 **Discussion**

286 In this study, we aimed to assess whether the antibody binding specificities to SARS-CoV-2
287 Spike in macaques are a useful model for the human response. Our results indicate important
288 similarities between macaques and humans; for example, both have antibodies that recognize
289 major epitopes in the CTD, FP, and SH-H. However, many differences are also apparent, with
290 some groups showing responses to unique epitopes, such as two physically proximal epitopes in
291 the NTD and CTD that are recognized by antibodies from vaccinated humans but not macaques.
292 Additionally, epitope regions flanking the FP were recognized by antibodies from convalescent
293 macaques, while antibodies from convalescent humans did not recognize the flanking regions

294 but showed a strong response within the FP itself. We found considerable diversity in the
295 pathways of escape between individuals, and this was not specific to either macaques or
296 humans, suggesting a diverse repertoire of antibodies that can respond to the major epitopes in
297 both groups. Overall, these results suggest that macaques and humans share recognition of
298 certain major epitopes. The differences that exist could be due to species (macaque vs. human),
299 but could also be influenced by differences in the specific type and number of exposures to
300 antigen in each group.

301 Other studies have characterized human monoclonal antibodies against some of the epitopes
302 we report here, many of them with neutralizing or other activities. As previously reported by
303 our group [60], we found that antibodies from vaccinated humans bound peptides spanning a
304 30 amino acid segment at the C-terminus of the NTD. Interestingly, most if not all neutralizing
305 human mAbs targeting the SARS-CoV-2 NTD to date have been shown to target a single
306 supersite on the “tip” of Spike, distinct from the epitope we detected at the C-terminus [49, 64-
307 70]. An NTD mAb with Fc effector function [71], as well as several NTD mAbs that enhance
308 infection in vitro [65, 72], also bind sites upstream of the C-terminal epitope. Therefore, future
309 studies are warranted to investigate the function of antibodies binding the new NTD epitope
310 detected by Phage-DMS. In the CTD, we detected broad antibody binding, with vaccinated
311 macaques, vaccinated humans, and convalescent macaques enriching peptides in the CTD-N’
312 epitope region, and vaccinated humans also recognizing peptides spanning the remainder of
313 this domain (CTD-C’). Polyclonal antibodies targeting sites within the CTD-N’ and CTD-C’ have
314 been isolated from human sera and shown to have neutralizing activity [73]. Interestingly, the
315 neutralizing epitope on the CTD-C’ (AA 625-636) [73] is physically adjacent to the NTD epitope

316 we describe (AA 285-305), raising the possibility that a conformational epitope extending to the
317 NTD is recognized by neutralizing antibodies from vaccinated humans. Depleting human serum
318 of FP-binding antibodies reduced its neutralization capacity [74]; these antibodies are of high
319 interest, both due to their potential to block membrane fusion, and given the high sequence
320 conservation among the FPs of diverse coronaviruses [75, 76]. We found that convalescent
321 rhesus macaque sera strongly recognized the pre- and post-FP epitope regions, but to our
322 knowledge, functional antibodies against these regions have not been previously described.
323 Finally, the SH-H epitope region we describe is in the stem helix, a region known to be highly
324 conserved across coronaviruses. Broadly neutralizing [77-79] stem helix antibodies have been
325 isolated and suggest an avenue for rational design of a pan-coronavirus vaccine. Interestingly, a
326 mAb raised against the MERS-CoV stem region protected mice against SARS-CoV-2 challenge,
327 despite having no neutralizing activity against SARS-CoV-2 in vitro [80]. The detection of broad
328 antibody binding across Spike supports the continued investigation of non-RBD epitopes, which
329 remain understudied. Some of the epitopes we describe may also be the target of non-
330 neutralizing Fc-effector antibodies [81], and/or antibodies that enhance infection via Fc-
331 independent [72] or Fc-dependent [82] mechanisms. This latter concept may be important in
332 the pathogenesis of COVID-19, though this remains speculative.

333 Previous work elucidated that pathways of antibody escape to SARS-CoV-2 Spike protein can be
334 quite variable in convalescent humans, with vaccination inducing a more consistent response
335 [60]. In the current study, we found considerable variability in escape profiles in the FP and
336 CTD-N' in both macaques and humans, though the convalescent rhesus macaques had more
337 concordant escape profiles than other groups. Variability in escape patterns suggests that a

338 diversity of antibodies are targeting these epitopes. Intra-species germline diversity in
339 immunoglobulin genes may help explain why individuals with similar exposures often mount
340 distinct responses [83, 84]. On the other hand, escape profiles were more consistent in the SH-
341 H, where the responses of convalescent macaques and vaccinated humans appeared to
342 converge. This conservation of response suggests that highly similar antibodies are dominating
343 the antibody repertoire against this epitope. Convergent antibody responses to SARS-CoV-2
344 have been reported within human populations [85-87], and our findings here suggest that
345 antibodies from different species may also be able to converge on the same “public” antibody
346 repertoires in a functional sense, despite genetic differences. While a shared escape profile
347 among individuals could suggest that viral escape mutations are more likely to emerge on a
348 population level, another factor to consider is the effect of the mutations on viral fitness. Key
349 domains of the S2 subunit (such as the SH-H epitope) have essential functions and high
350 sequence conservation, suggesting a low tolerance for mutation and thus for escape. Indeed,
351 previous work determined that sites of escape identified by Phage-DMS are not typically
352 mutated at a high frequency in circulating strains of SARS-CoV-2 [59].

353 While our focus was on understanding how macaques and humans respond to a similar
354 exposure (i.e., vaccination or infection), we also noted similarities in response between re-
355 infected macaques and vaccinated humans. These groups both exhibited the broadest
356 recognition across Spike, although the epitope regions they targeted were somewhat different.
357 As described above, these groups also had highly similar antibody escape profiles in the SH-H.
358 The vaccinated humans and re-infected macaques both received two exposures to high doses
359 of antigen. It is plausible that re-exposure directed initially diverse antibodies to converge on a

360 more focused response in both scenarios. While it is known that vaccination and infection
361 induce distinct humoral responses against Spike [60, 88, 89], our data suggest that a second
362 exposure may generate antibodies that better match the vaccine-induced response.
363 This study had several limitations. Because the Phage-DMS library displays peptides 31AA in
364 length, discontinuous or conformational epitopes are not readily detected using this method.
365 Additionally, epitopes that may normally be glycosylated are exposed for antibody binding in
366 Phage-DMS. There also are known germline-encoded differences in the properties of
367 immunoglobulin subclasses and Fc receptors between macaques and humans, leading to
368 differences in antibody function that cannot be assayed using Phage-DMS [90]. Additionally,
369 our sample set includes variables that limit our ability to draw conclusions about species-
370 specific (macaque vs. human) differences in antibody response. The vaccinated macaques and
371 humans both received RNA vaccines encoding full-length Spike protein, but there were
372 differences in vaccine technology, including: 1) the use of mRNA in the human vaccine vs.
373 repRNA in the macaque vaccine, 2) the stabilization of Spike in its pre-fusion state in the human
374 vaccine, 3) the dosage and number of doses delivered, and 4) the formulation used to deliver
375 the RNA. Despite these differences, we found commonalities in some of the epitopes targeted
376 by antibodies from both groups. Additionally, the convalescent rhesus macaques were
377 experimentally infected twice with high titers of virus, compared to the convalescent humans
378 who were naturally infected once. This important discrepancy could be the reason why the
379 response in re-infected macaques aligned more closely with vaccinated humans than
380 convalescent humans. Studies of re-infected humans would help address this possibility.

381 Our findings suggest that while vaccinated and convalescent macaques and humans share
382 recognition of some major epitopes, each group has a unique antibody binding profile.
383 Antibody escape profiles suggest a diversity of individual responses to most epitopes.
384 Important avenues for future study include comparing macaque and human responses to the
385 RBD and evaluating species differences in antibody function. Continued investigation of
386 immunogenic epitopes in conserved regions of Spike is also warranted to inform the
387 development of immunity that is more robust in the face of viral escape.

388 **Materials and Methods**

389 **Samples**

390 **Vaccinated pigtail macaques**

391 Plasma was collected from 11 pigtail macaques immunized with a replicating RNA (repRNA)
392 vaccine expressing full-length SARS-CoV-2 Spike protein. A subset of these animals was
393 previously described [35]. All animals were housed at the Washington National Primate
394 Research Center (WaNPRC), an accredited facility of the American Association for the
395 Accreditation of Laboratory Animal Care International (AAALAC). All procedures were
396 approved by the University of Washington's Institutional Animal Care and Use Committee
397 (IACUC) (IACUC #4266-14). Individual macaques received the vaccine by intramuscular
398 injection in either a Lipid InOrganic Nanoparticle (LION) [35] or a Nanostructured Lipid Carrier
399 (NLC) [61] formulation, delivered in a single priming dose of 25ug (n=3) or 250ug (n=6) or in a
400 prime-boost regimen with 50ug doses spaced 4 weeks apart (n=2). All samples were collected 6

401 weeks post-prime immunization. A subset of these animals also previously received an
402 experimental hepatitis B vaccine as part of another study (n=5).

403 **Convalescent rhesus macaques**

404 Serum was collected from 12 rhesus macaques housed at the Rocky Mountain Laboratories
405 (National Institutes of Health [NIH]), 14 days after the second of two SARS-CoV-2 infections
406 spaced 42 days apart. Prior to infection, macaques were variably depleted of CD4+ T cells, CD8+
407 T cells, CD4+ and CD8+ T cells, or neither, as part of another study. Details of macaque
408 treatment and regulatory approvals are as published previously [39].

409 **Vaccinated humans**

410 We obtained serum from 15 individuals who received two 100ug doses of the Moderna mRNA-
411 1273 vaccine as part of a phase I clinical trial (NCT04283461) [91]. Phage-DMS results from
412 these samples were reported previously [60]. Because samples were de-identified, this study
413 was approved by the Fred Hutchinson Cancer Research Center Institutional Review Board as
414 nonhuman subjects research. Only samples from individuals aged 18-55 years were included in
415 the current study to better match the young age range of the macaques.

416 **Convalescent humans**

417 Plasma was collected from 12 individuals post-mild COVID-19 illness as part of the Hospitalized
418 or Ambulatory Adults with Respiratory Viral Infections (HAARVI) study in Seattle, WA. Phage-
419 DMS results from these samples were reported previously [59, 60]. This research was approved
420 by the University of Washington Institutional Review Board (IRB number STUDY00000959).
421 Again, the sample set was restricted to only include individuals aged 18-55 years to better
422 match other sample groups.

423 All plasma and sera were heat inactivated at 56°C for 1 hour prior to use. Full details of all
424 samples are available in Tables 1 and S1.

425 **Phage-DMS, Illumina library preparation and deep sequencing**

426 The experimental protocol was performed exactly as described previously [59]. Briefly, an
427 oligonucleotide pool was synthesized that contains sequences coding for peptides of 31 amino
428 acids that tile along the length of the Wuhan-Hu-1 Spike protein sequence [92] in 1 amino acid
429 increments. For each peptide with the wildtype sequence, 19 variations were included that
430 have a single mutation at the middle amino acid, resulting in a total library size of 24,820
431 unique sequences. The oligonucleotide pool was cloned into T7 phage, followed by
432 amplification of the phage library; this step was performed twice independently to generate
433 biological duplicate phage libraries. The phage library was incubated with a serum or plasma
434 sample, then bound antibody-phage complexes were immunoprecipitated using Protein A and
435 Protein G Dynabeads (Invitrogen). Bound phage were lysed, and DNA was amplified by PCR and
436 cleaned prior to sequencing on an Illumina MiSeq or HiSeq 2500 with single end reads.
437 Demultiplexing and read alignment were also performed as described previously [60].

438 **Replicate curation**

439 Biological replicates were analyzed in parallel to assess reproducibility of results. For simplicity,
440 results from only one biological replicate are shown and described, with the same figures
441 generated with the second biological replicate available to view online at
442 <https://github.com/matsengrp/phage-dms-nhp-analysis>. Within each biological replicate, “in-

443 line” technical replicates were run for some samples. In these cases, the technical replicate with
444 the highest mapped read count was selected for analysis.

445 **Wildtype enrichment and defining epitope regions**

446 The enrichment of wildtype peptides was calculated as described previously to quantify the
447 proportion of each peptide in an antibody-selected sample relative to the proportion of that
448 peptide in the input phage library [58]. On enrichment plots, the locus of each peptide is
449 defined by its middle amino acid. Enrichment values of wildtype peptides were summed across
450 epitope regions of interest for statistical comparisons between groups (“Summed WT
451 enrichment” on figures). Mann-Whitney U tests were performed with multiple comparisons
452 adjustment using the Bonferroni-Dunn method.

453 **Escape profile comparison**

454 The effect of a mutation on antibody-peptide binding was quantified as “differential selection,”
455 which is the log fold change in the enrichment of a mutation-containing peptide compared to
456 the wildtype peptide. This number is multiplied by the average of the wildtype peptide
457 enrichments at that site and its two adjacent sites to get a “scaled differential selection” value,
458 as described previously [60]. The enrichment values of the adjacent wildtype peptides are
459 included in this calculation to make the analysis less susceptible to noise. Negative differential
460 selection values represent reduced binding compared to wildtype, while positive differential
461 selection values indicate that the mutation enhanced binding. “Summed differential selection”
462 is the sum of the 19 scaled differential selection values for all mutations at a site, and gives a
463 sense of the overall magnitude of escape at that site.

464 The comparison of two escape profiles is quantified by an escape similarity score computed in
465 the framework of an optimal transport problem [93]; this algorithm was described in detail at
466 <https://matsengrp.github.io/phipperry/esc-prof.html>. An overview of the method is shown in S4
467 Fig. Escape profiles are commonly portrayed as logo plots using scaled differential selection
468 values (S4A Fig). At each site, escape data in logo plot form can instead be represented as
469 binned distributions, with each mutation making some contribution to the total amount of
470 escape at that site based on its scaled differential selection value (S4B Fig). For each site, an
471 optimal transport problem computes the most efficient way to transform one individual's
472 escape distribution into that of a different individual (S4C Fig). The cost to "exchange" amino
473 acid contributions between profiles is based on the similarity between the amino acids being
474 exchanged, as defined by the BLOSUM62 matrix [94]. More "movement" between dissimilar
475 amino acids drives up the total cost of the transport; therefore, a higher cost indicates less
476 similar profiles. Escape similarity scores are the inverse of the total cost of transforming one
477 profile into another. Scores were calculated between pairwise combinations of individuals to
478 compare escape profile variability within and between sample groups.

479 **Protein structure**

480 The structure of a SARS-CoV-2 Spike glycoprotein monomer in the closed state (PDB 6XR8) was
481 examined to visualize epitope regions [95]. Coloring was added using UCSF ChimeraX-1.2.5,
482 developed by the Resource for Biocomputing, Visualization, and Informatics at the University of
483 California, San Francisco, with support from National Institutes of Health R01-GM129325 and
484 the Office of Cyber Infrastructure and Computational Biology, National Institute of Allergy and
485 Infectious Diseases [96].

486 **Code, software, and data availability**

487 All analyses were performed in RStudio version 1.3.1093, Python version 3.6.12, GraphPad
488 Prism version 9.0.1, and the phip-flow and phipperry software suite
489 (<https://matsengrp.github.io/phipperry/>). The phip-flow tools perform read alignment using
490 Bowtie2 [97] in a Nextflow [98] pipeline script. The escape profile comparisons are done with
491 phipperry in Python 3.6.12 and depend on the NumPy [99], pandas [100, 101], xarray [102], POT
492 [103], and biopython [104] packages. All code and instructions for running this analysis are
493 available at <https://github.com/matsengrp/phage-dms-nhp-analysis>.

494 **Acknowledgements**

495 We thank Caitlin Stoddard for helpful guidance on the analysis and interpretation of our results.
496 We are also grateful to Cassie Sather and others at the Genomics core facility for assistance
497 with sequencing. We thank Lisa Jackson (Kaiser Permanente), Chris Roberts, Catherine Luke,
498 and Rebecca Lampley [National Institute of Allergy and Infectious Diseases (NIAID), NIH] for
499 assistance obtaining the mRNA-1273 phase 1 trial vaccine samples (NCT04283461). We thank
500 all volunteers in the phase 1 trial, as well as all research participants and study staff of the
501 Hospitalized or Ambulatory Adults with Respiratory Viral Infections (HAARVI) study, without
502 whom this work would not be possible.

503
504
505
506
507
508
509
510
511
512
513
514
515
516
517
518
519
520
521
522
523

REFERENCES

1. Corbett KS, Flynn B, Foulds KE, Francica JR, Boyoglu-Barnum S, Werner AP, et al. Evaluation of the mRNA-1273 Vaccine against SARS-CoV-2 in Nonhuman Primates. *N Engl J Med.* 2020; 383(16):1544-1555.
2. Vogel AB, Kanevsky I, Che Y, Swanson KA, Muik A, Vormehr M, et al. BNT162b vaccines protect rhesus macaques from SARS-CoV-2. *Nature.* 2021; 592(7853):283-289.
3. Mercado NB, Zahn R, Wegmann F, Loos C, Chandrashekar A, Yu J, et al. Single-shot Ad26 vaccine protects against SARS-CoV-2 in rhesus macaques. *Nature.* 2020; 586(7830):583-588.
4. van Doremalen N, Lambe T, Spencer A, Belij-Rammerstorfer S, Purushotham JN, Port JR, et al. ChAdOx1 nCoV-19 vaccine prevents SARS-CoV-2 pneumonia in rhesus macaques. *Nature.* 2020; 586(7830):578-582.
5. Gao Q, Bao L, Mao H, Wang L, Xu K, Yang M, et al. Development of an inactivated vaccine candidate for SARS-CoV-2. *Science.* 2020; 369(6499):77-81.
6. Yu J, Tostanoski LH, Peter L, Mercado NB, McMahan K, Mahrokhian SH, et al. DNA vaccine protection against SARS-CoV-2 in rhesus macaques. *Science.* 2020; 369(6505):806-811.
7. Yang J, Wang W, Chen Z, Lu S, Yang F, Bi Z, et al. A vaccine targeting the RBD of the S protein of SARS-CoV-2 induces protective immunity. *Nature.* 2020; 586(7830):572-577.
8. Wang H, Zhang Y, Huang B, Deng W, Quan Y, Wang W, et al. Development of an Inactivated Vaccine Candidate, BBIBP-CorV, with Potent Protection against SARS-CoV-2. *Cell.* 2020; 182(3):713-721.e9.

- 524 9. Feng L, Wang Q, Shan C, Yang C, Feng Y, Wu J, et al. An adenovirus-vectored COVID-19
525 vaccine confers protection from SARS-COV-2 challenge in rhesus macaques. *Nat Commun.*
526 2020; 11:1-11.
- 527 10. Ma X, Zou F, Yu F, Li R, Yuan Y, Zhang Y, et al. Nanoparticle Vaccines Based on the
528 Receptor Binding Domain (RBD) and Heptad Repeat (HR) of SARS-CoV-2 Elicit Robust Protective
529 Immune Responses. *Immunity.* 2020; 53(6):1315-1330.e9.
- 530 11. Sui Y, Li J, Zhang R, Prabhu SK, Andersen H, Venzon D, et al. Protection against SARS-
531 CoV-2 infection by a mucosal vaccine in rhesus macaques. *JCI Insight.* 2021; 6(10):e148494.
- 532 12. Harris PE, Brasel T, Massey C, Herst CV, Burkholz S, Lloyd P, et al. A Synthetic Peptide
533 CTL Vaccine Targeting Nucleocapsid Confers Protection from SARS-CoV-2 Challenge in Rhesus
534 Macaques. *Vaccines (Basel).* 2021; 9(5):520.
- 535 13. Yadav PD, Ella R, Kumar S, Patil DR, Mohandas S, Shete AM, et al. Immunogenicity and
536 protective efficacy of inactivated SARS-CoV-2 vaccine candidate, BBV152 in rhesus macaques.
537 *Nat Commun.* 2021; 12(1):1386.
- 538 14. Garrido C, Curtis AD, 2nd, Dennis M, Pathak SH, Gao H, Montefiori D, et al. SARS-CoV-2
539 vaccines elicit durable immune responses in infant rhesus macaques. *Sci Immunol.* 2021;
540 6(60):eabj3684.
- 541 15. Routhu NK, Cheedarla N, Gangadhara S, Bollimpelli VS, Boddapati AK, Shiferaw A, et al.
542 A modified vaccinia Ankara vector-based vaccine protects macaques from SARS-CoV-2
543 infection, immune pathology, and dysfunction in the lungs. *Immunity.* 2021; 54(3):542-556.e9.

- 544 16. Li H, Guo L, Zheng H, Li J, Zhao X, Li J, et al. Self-Assembling Nanoparticle Vaccines
545 Displaying the Receptor Binding Domain of SARS-CoV-2 Elicit Robust Protective Immune
546 Responses in Rhesus Monkeys. *Bioconjug Chem.* 2021; 32(5):1034-1046.
- 547 17. Li Y, Bi Y, Xiao H, Yao Y, Liu X, Hu Z, et al. A novel DNA and protein combination COVID-
548 19 vaccine formulation provides full protection against SARS-CoV-2 in rhesus macaques. *Emerg*
549 *Microbes Infect.* 2021; 10(1):342-355.
- 550 18. Arunachalam PS, Walls AC, Golden N, Atyeo C, Fischinger S, Li C, et al. Adjuvanting a
551 subunit COVID-19 vaccine to induce protective immunity. *Nature.* 2021; 594(7862):253-258.
- 552 19. Liang JG, Su D, Song TZ, Zeng Y, Huang W, Wu J, et al. S-Trimer, a COVID-19 subunit
553 vaccine candidate, induces protective immunity in nonhuman primates. *Nat Commun.* 2021;
554 12(1):1346.
- 555 20. Luo S, Zhang P, Liu B, Yang C, Liang C, Wang Q, et al. Prime-boost vaccination of mice
556 and rhesus macaques with two novel adenovirus vectored COVID-19 vaccine candidates. *Emerg*
557 *Microbes Infect.* 2021; 10(1):1002-1015.
- 558 21. Solfrosi L, Kuipers H, Jongeneelen M, Rosendahl Huber SK, van der Lubbe JEM, Dekking
559 L, et al. Immunogenicity and efficacy of one and two doses of Ad26.COV2.S COVID vaccine in
560 adult and aged NHP. *J Exp Med.* 2021; 218(7):e20202756.
- 561 22. Walls AC, Miranda MC, Schafer A, Pham MN, Greaney A, Arunachalam PS, et al.
562 Elicitation of broadly protective sarbecovirus immunity by receptor-binding domain
563 nanoparticle vaccines. *Cell.* 2021; 184(21):5432-5447.e16.

- 564 23. King HAD, Joyce MG, Lakhal-Naouar I, Ahmed A, Cincotta CM, Subra C, et al. Efficacy and
565 breadth of adjuvanted SARS-CoV-2 receptor-binding domain nanoparticle vaccine in macaques.
566 Proc Natl Acad Sci U S A. 2021; 118(38):e2106433118.
- 567 24. Guebre-Xabier M, Patel N, Tian JH, Zhou B, Maciejewski S, Lam K, et al. NVX-CoV2373
568 vaccine protects cynomolgus macaque upper and lower airways against SARS-CoV-2 challenge.
569 Vaccine. 2020; 38(50):7892-7896.
- 570 25. Sanchez-Felipe L, Vercruyse T, Sharma S, Ma J, Lemmens V, Van Looveren D, et al. A
571 single-dose live-attenuated YF17D-vectored SARS-CoV-2 vaccine candidate. Nature. 2021;
572 590(7845):320-325.
- 573 26. Zhang NN, Li XF, Deng YQ, Zhao H, Huang YJ, Yang G, et al. A Thermostable mRNA
574 Vaccine against COVID-19. Cell. 2020; 182(5):1271-1283.e16.
- 575 27. Li T, Zheng Q, Yu H, Wu D, Xue W, Xiong H, et al. SARS-CoV-2 spike produced in insect
576 cells elicits high neutralization titres in non-human primates. Emerg Microbes Infect. 2020;
577 9(1):2076-2090.
- 578 28. Brouwer PJM, Brinkkemper M, Maisonnasse P, Dereuddre-Bosquet N, Grobben M,
579 Claireaux M, et al. Two-component spike nanoparticle vaccine protects macaques from SARS-
580 CoV-2 infection. Cell. 2021; 184(5):1188-1200.e19.
- 581 29. Hong SH, Oh H, Park YW, Kwak HW, Oh EY, Park HJ, et al. Immunization with RBD-P2 and
582 N protects against SARS-CoV-2 in nonhuman primates. Sci Adv. 2021; 7(22):eabg7156.
- 583 30. Sun S, He L, Zhao Z, Gu H, Fang X, Wang T, et al. Recombinant vaccine containing an
584 RBD-Fc fusion induced protection against SARS-CoV-2 in nonhuman primates and mice. Cell Mol
585 Immunol. 2021; 18(4):1070-1073.

- 586 31. Capone S, Raggioli A, Gentile M, Battella S, Lahm A, Sommella A, et al. Immunogenicity
587 of a new gorilla adenovirus vaccine candidate for COVID-19. *Mol Ther.* 2021; 29(8):2412-2423.
- 588 32. Kalnin KV, Plitnik T, Kishko M, Zhang J, Zhang D, Beauvais A, et al. Immunogenicity and
589 efficacy of mRNA COVID-19 vaccine MRT5500 in preclinical animal models. *NPJ Vaccines.* 2021;
590 6(1):61.
- 591 33. Walls AC, Fiala B, Schafer A, Wrenn S, Pham MN, Murphy M, et al. Elicitation of Potent
592 Neutralizing Antibody Responses by Designed Protein Nanoparticle Vaccines for SARS-CoV-2.
593 *Cell.* 2020; 183(5):1367-1382.e17.
- 594 34. Tan HX, Juno JA, Lee WS, Barber-Axthelm I, Kelly HG, Wragg KM, et al. Immunogenicity
595 of prime-boost protein subunit vaccine strategies against SARS-CoV-2 in mice and macaques.
596 *Nat Commun.* 2021; 12(1):1403.
- 597 35. Erasmus JH, Khandhar AP, O'Connor MA, Walls AC, Hemann EA, Murapa P, et al. An
598 Alphavirus-derived replicon RNA vaccine induces SARS-CoV-2 neutralizing antibody and T cell
599 responses in mice and nonhuman primates. *Sci Transl Med.* 2020; 12(555):eabc9396.
- 600 36. Hewitt JA, Lutz C, Florence WC, Pitt MLM, Rao S, Rappaport J, et al. ACTIVating
601 Resources for the COVID-19 Pandemic: In Vivo Models for Vaccines and Therapeutics. *Cell Host*
602 *Microbe.* 2020; 28(5):646-659.
- 603 37. Deng W, Bao L, Liu J, Xiao C, Liu J, Xue J, et al. Primary exposure to SARS-CoV-2 protects
604 against reinfection in rhesus macaques. *Science.* 2020; 369(6505):818-823.
- 605 38. Chandrashekar A, Liu J, Martinot AJ, McMahan K, Mercado NB, Peter L, et al. SARS-CoV-
606 2 infection protects against rechallenge in rhesus macaques. *Science.* 2020; 369(6505):812-817.

- 607 39. Hasenkrug KJ, Feldmann F, Myers L, Santiago ML, Guo K, Barrett BS, et al. Recovery from
608 Acute SARS-CoV-2 Infection and Development of Anamnestic Immune Responses in T Cell-
609 Depleted Rhesus Macaques. *mBio*. 2021; 12(4):e0150321.
- 610 40. Walls AC, Park YJ, Tortorici MA, Wall A, McGuire AT, Velesler D. Structure, Function, and
611 Antigenicity of the SARS-CoV-2 Spike Glycoprotein. *Cell*. 2020; 181(2):281-292.e6.
- 612 41. Wrapp D, Wang N, Corbett KS, Goldsmith JA, Hsieh CL, Abiona O, et al. Cryo-EM
613 structure of the 2019-nCoV spike in the prefusion conformation. *Science*. 2020;
614 367(6483):1260-1263.
- 615 42. Li F. Structure, Function, and Evolution of Coronavirus Spike Proteins. *Annu Rev Virol*.
616 2016; 3(1):237-261.
- 617 43. Fan X, Cao D, Kong L, Zhang X. Cryo-EM analysis of the post-fusion structure of the SARS-
618 CoV spike glycoprotein. *Nat Commun*. 2020; 11(1):3618.
- 619 44. Khoury DS, Cromer D, Reynaldi A, Schlub TE, Wheatley AK, Juno JA, et al. Neutralizing
620 antibody levels are highly predictive of immune protection from symptomatic SARS-CoV-2
621 infection. *Nat Med*. 2021; 27(7):1205-1211.
- 622 45. Lumley SF, O'Donnell D, Stoesser NE, Matthews PC, Howarth A, Hatch SB, et al. Antibody
623 Status and Incidence of SARS-CoV-2 Infection in Health Care Workers. *N Engl J Med*. 2021;
624 384(6):533-540.
- 625 46. Corbett KS, Nason MC, Flach B, Gagne M, O'Connell S, Johnston TS, et al. Immune
626 correlates of protection by mRNA-1273 vaccine against SARS-CoV-2 in nonhuman primates.
627 *Science*. 2021; 373(6561):eabj0299.

- 628 47. Gilbert PB, Montefiori DC, McDermott A, Fong Y, Benkeser DC, Deng W, et al. Immune
629 Correlates Analysis of the mRNA-1273 COVID-19 Vaccine Efficacy Trial. medRxiv [Preprint]. 2021
630 [cited 2021 Nov 10]. doi: 10.1101/2021.08.09.21261290.
- 631 48. Rogers TF, Zhao F, Huang D, Beutler N, Burns A, He WT, et al. Isolation of potent SARS-
632 CoV-2 neutralizing antibodies and protection from disease in a small animal model. *Science*.
633 2020; 369(6506):956-963.
- 634 49. Voss WN, Hou YJ, Johnson NV, Delidakis G, Kim JE, Javanmardi K, et al. Prevalent,
635 protective, and convergent IgG recognition of SARS-CoV-2 non-RBD spike epitopes. *Science*.
636 2021; 372(6546):1108-1112.
- 637 50. Greaney AJ, Loes AN, Crawford KHD, Starr TN, Malone KD, Chu HY, et al. Comprehensive
638 mapping of mutations in the SARS-CoV-2 receptor-binding domain that affect recognition by
639 polyclonal human plasma antibodies. *Cell Host Microbe*. 2021; 29(3):463-476.e6.
- 640 51. Harvey WT, Carabelli AM, Jackson B, Gupta RK, Thomson EC, Harrison EM, et al. SARS-
641 CoV-2 variants, spike mutations and immune escape. *Nat Rev Microbiol*. 2021; 19(7):409-424.
- 642 52. Schafer A, Muecksch F, Lorenzi JCC, Leist SR, Cipolla M, Bournazos S, et al. Antibody
643 potency, effector function, and combinations in protection and therapy for SARS-CoV-2
644 infection in vivo. *J Exp Med*. 2021; 218(3):e20201993.
- 645 53. Winkler ES, Gilchuk P, Yu J, Bailey AL, Chen RE, Chong Z, et al. Human neutralizing
646 antibodies against SARS-CoV-2 require intact Fc effector functions for optimal therapeutic
647 protection. *Cell*. 2021; 184(7):1804-1820.e16.

- 648 54. Gorman MJ, Patel N, Guebre-Xabier M, Zhu AL, Atyeo C, Pullen KM, et al. Fab and Fc
649 contribute to maximal protection against SARS-CoV-2 following NVX-CoV2373 subunit vaccine
650 with Matrix-M vaccination. *Cell Rep Med*. 2021; 2(9):100405.
- 651 55. Tauzin A, Nayrac M, Benlarbi M, Gong SY, Gasser R, Beaudoin-Bussieres G, et al. A single
652 dose of the SARS-CoV-2 vaccine BNT162b2 elicits Fc-mediated antibody effector functions and T
653 cell responses. *Cell Host Microbe*. 2021; 29(7):1137-1150.e6.
- 654 56. Ullah I, Prevost J, Ladinsky MS, Stone H, Lu M, Anand SP, et al. Live imaging of SARS-CoV-
655 2 infection in mice reveals that neutralizing antibodies require Fc function for optimal efficacy.
656 *Immunity*. 2021; 54(9):2143-2158.e15.
- 657 57. Brunet-Ratnasingham E, Anand SP, Gantner P, Moquin-Beaudry G, Dyachenko A,
658 Brassard N, et al. Integrated immunovirological profiling validates plasma SARS-CoV-2 RNA
659 as an early predictor of COVID-19 mortality. *medRxiv [Preprint]*. 2021 [cited 2021 Nov 10]. doi:
660 10.1101/2021.03.18.21253907.
- 661 58. Garrett ME, Itell HL, Crawford KHD, Basom R, Bloom JD, Overbaugh J. Phage-DMS: A
662 Comprehensive Method for Fine Mapping of Antibody Epitopes. *iScience*. 2020; 23(10):101622.
- 663 59. Garrett ME, Galloway J, Chu HY, Itell HL, Stoddard CI, Wolf CR, et al. High-resolution
664 profiling of pathways of escape for SARS-CoV-2 spike-binding antibodies. *Cell*. 2021;
665 184(11):2927-2938.e11.
- 666 60. Garrett ME, Galloway JG, Wolf C, Logue JK, Franko N, Chu HY, et al. Comprehensive
667 characterization of the antibody responses to SARS-CoV-2 Spike protein after infection and/or
668 vaccination. *bioRxiv [Preprint]*. 2021 [cited 2021 Nov 10]. doi: 10.1101/2021.10.05.463210.

- 669 61. Erasmus JH, Khandhar AP, Guderian J, Granger B, Archer J, Archer M, et al. A
670 Nanostructured Lipid Carrier for Delivery of a Replicating Viral RNA Provides Single, Low-Dose
671 Protection against Zika. *Mol Ther.* 2018; 26(10):2507-2522.
- 672 62. Yuan M, Liu H, Wu NC, Wilson IA. Recognition of the SARS-CoV-2 receptor binding
673 domain by neutralizing antibodies. *Biochem Biophys Res Commun.* 2021; 538:192-203.
- 674 63. Niu L, Wittrock KN, Clabaugh GC, Srivastava V, Cho MW. A Structural Landscape of
675 Neutralizing Antibodies Against SARS-CoV-2 Receptor Binding Domain. *Front Immunol.* 2021;
676 12:647934.
- 677 64. Chi X, Yan R, Zhang J, Zhang G, Zhang Y, Hao M, et al. A neutralizing human antibody
678 binds to the N-terminal domain of the Spike protein of SARS-CoV-2. *Science.* 2020;
679 369(6504):650-655.
- 680 65. Li D, Edwards RJ, Manne K, Martinez DR, Schafer A, Alam SM, et al. In vitro and in vivo
681 functions of SARS-CoV-2 infection-enhancing and neutralizing antibodies. *Cell.* 2021;
682 184(16):4203-4219.e32.
- 683 66. Liu L, Wang P, Nair MS, Yu J, Rapp M, Wang Q, et al. Potent neutralizing antibodies
684 against multiple epitopes on SARS-CoV-2 spike. *Nature.* 2020; 584(7821):450-456.
- 685 67. Wang N, Sun Y, Feng R, Wang Y, Guo Y, Zhang L, et al. Structure-based development of
686 human antibody cocktails against SARS-CoV-2. *Cell Res.* 2021; 31(1):101-103.
- 687 68. Cerutti G, Guo Y, Zhou T, Gorman J, Lee M, Rapp M, et al. Potent SARS-CoV-2
688 neutralizing antibodies directed against spike N-terminal domain target a single supersite. *Cell*
689 *Host Microbe.* 2021; 29(5):819-833.e7.

- 690 69. McCallum M, De Marco A, Lempp FA, Tortorici MA, Pinto D, Walls AC, et al. N-terminal
691 domain antigenic mapping reveals a site of vulnerability for SARS-CoV-2. *Cell*. 2021;
692 184(9):2332-2347.e16.
- 693 70. Suryadevara N, Shrihari S, Gilchuk P, VanBlargan LA, Binshtein E, Zost SJ, et al.
694 Neutralizing and protective human monoclonal antibodies recognizing the N-terminal domain
695 of the SARS-CoV-2 spike protein. *Cell*. 2021; 184(9):2316-2331.e15.
- 696 71. Beaudoin-Bussi eres G, Chen Y, Ullah I, Pr evost J, Tolbert WD, Symmes K, et al. An anti-
697 SARS-CoV-2 non-neutralizing antibody with Fc-effector function defines a new NTD epitope and
698 delays neuroinvasion and death in K18-hACE2 mice. *bioRxiv [Preprint]*. 2021 [cited 2021 Nov
699 10]. doi: 10.1101/2021.09.08.459408.
- 700 72. Liu Y, Soh WT, Kishikawa JI, Hirose M, Nakayama EE, Li S, et al. An infectivity-enhancing
701 site on the SARS-CoV-2 spike protein targeted by antibodies. *Cell*. 2021; 184(13):3452-
702 3466.e18.
- 703 73. Li Y, Lai DY, Zhang HN, Jiang HW, Tian X, Ma ML, et al. Linear epitopes of SARS-CoV-2
704 spike protein elicit neutralizing antibodies in COVID-19 patients. *Cell Mol Immunol*. 2020;
705 17(10):1095-1097.
- 706 74. Poh CM, Carissimo G, Wang B, Amrun SN, Lee CY, Chee RS, et al. Two linear epitopes on
707 the SARS-CoV-2 spike protein that elicit neutralising antibodies in COVID-19 patients. *Nat*
708 *Commun*. 2020; 11(1):2806.
- 709 75. Tang T, Bidon M, Jaimes JA, Whittaker GR, Daniel S. Coronavirus membrane fusion
710 mechanism offers a potential target for antiviral development. *Antiviral Res*. 2020; 178:104792.

- 711 76. Madu IG, Roth SL, Belouzard S, Whittaker GR. Characterization of a highly conserved
712 domain within the severe acute respiratory syndrome coronavirus spike protein S2 domain with
713 characteristics of a viral fusion peptide. *J Virol.* 2009; 83(15):7411-7421.
- 714 77. Zhou P, Yuan M, Song G, Beutler N, Shaabani N, Huang D, et al. A protective broadly
715 cross-reactive human antibody defines a conserved site of vulnerability on beta-coronavirus
716 spikes. *bioRxiv [Preprint]*. 2021 [cited 2021 Nov 10]. doi: 10.1101/2021.03.30.437769.
- 717 78. Pinto D, Sauer MM, Czudnochowski N, Low JS, Tortorici MA, Housley MP, et al. Broad
718 betacoronavirus neutralization by a stem helix-specific human antibody. *Science.* 2021;
719 373(6559):1109-1116.
- 720 79. Li W, Chen Y, Prévost J, Ullah I, Lu M, Gong SY, et al. Structural Basis and Mode of Action
721 for Two Broadly Neutralizing Antibodies Against SARS-CoV-2 Emerging Variants of Concern.
722 *bioRxiv [Preprint]*. 2021 [cited 2021 Nov 10]. doi: 10.1101/2021.08.02.454546.
- 723 80. Hsieh CL, Werner AP, Leist SR, Stevens LJ, Falconer E, Goldsmith JA, et al. Stabilized
724 coronavirus spike stem elicits a broadly protective antibody. *Cell Rep.* 2021; 37(5):109929.
- 725 81. Zohar T, Alter G. Dissecting antibody-mediated protection against SARS-CoV-2. *Nat Rev*
726 *Immunol.* 2020; 20(7):392-394.
- 727 82. Lee WS, Wheatley AK, Kent SJ, DeKosky BJ. Antibody-dependent enhancement and
728 SARS-CoV-2 vaccines and therapies. *Nat Microbiol.* 2020; 5(10):1185-1191.
- 729 83. Mikocziova I, Greiff V, Sollid LM. Immunoglobulin germline gene variation and its impact
730 on human disease. *Genes Immun.* 2021; 22(4):205-217.

- 731 84. Ramesh A, Darko S, Hua A, Overman G, Ransier A, Francica JR, et al. Structure and
732 Diversity of the Rhesus Macaque Immunoglobulin Loci through Multiple De Novo Genome
733 Assemblies. *Front Immunol.* 2017; 8:1407.
- 734 85. Robbiani DF, Gaebler C, Muecksch F, Lorenzi JCC, Wang Z, Cho A, et al. Convergent
735 antibody responses to SARS-CoV-2 in convalescent individuals. *Nature.* 2020; 584(7821):437-
736 442.
- 737 86. Chen EC, Gilchuk P, Zost SJ, Suryadevara N, Winkler ES, Cabel CR, et al. Convergent
738 antibody responses to the SARS-CoV-2 spike protein in convalescent and vaccinated individuals.
739 *Cell Rep.* 2021; 36(8):109604.
- 740 87. Nielsen SCA, Yang F, Jackson KJL, Hoh RA, Roltgen K, Jean GH, et al. Human B Cell Clonal
741 Expansion and Convergent Antibody Responses to SARS-CoV-2. *Cell Host Microbe.* 2020;
742 28(4):516-525.e5.
- 743 88. Greaney AJ, Loes AN, Gentles LE, Crawford KHD, Starr TN, Malone KD, et al. Antibodies
744 elicited by mRNA-1273 vaccination bind more broadly to the receptor binding domain than do
745 those from SARS-CoV-2 infection. *Sci Transl Med.* 2021; 13(600):eabi9915.
- 746 89. Amanat F, Thapa M, Lei T, Ahmed SMS, Adelsberg DC, Carreno JM, et al. SARS-CoV-2
747 mRNA vaccination induces functionally diverse antibodies to NTD, RBD, and S2. *Cell.* 2021;
748 184(15):3936-3948.e10.
- 749 90. Crowley AR, Ackerman ME. Mind the Gap: How Interspecies Variability in IgG and Its
750 Receptors May Complicate Comparisons of Human and Non-human Primate Effector Function.
751 *Front Immunol.* 2019; 10:697.

- 752 91. Jackson LA, Anderson EJ, Roupael NG, Roberts PC, Makhene M, Coler RN, et al. An
753 mRNA Vaccine against SARS-CoV-2 - Preliminary Report. *N Engl J Med.* 2020; 383(20):1920-
754 1931.
- 755 92. Wu F, Zhao S, Yu B, Chen YM, Wang W, Song ZG, et al. A new coronavirus associated
756 with human respiratory disease in China. *Nature.* 2020; 579(7798):265-269.
- 757 93. Monge G. Mémoire sur la théorie des déblais et des remblais. *Histoire de l'Académie*
758 *Royale des Sciences de Paris, avec les Mémoires de Mathématique et de Physique pour la*
759 *même année.* 1781:666-704.
- 760 94. Henikoff S, Henikoff JG. Amino acid substitution matrices from protein blocks. *Proc Natl*
761 *Acad Sci U S A.* 1992; 89(22):10915-10919.
- 762 95. Cai Y, Zhang J, Xiao T, Peng H, Sterling SM, Walsh RM, Jr., et al. Distinct conformational
763 states of SARS-CoV-2 spike protein. *Science.* 2020; 369(6511):1586-1592.
- 764 96. Pettersen EF, Goddard TD, Huang CC, Meng EC, Couch GS, Croll TI, et al. UCSF ChimeraX:
765 Structure visualization for researchers, educators, and developers. *Protein Sci.* 2021; 30(1):70-
766 82.
- 767 97. Langmead B, Salzberg SL. Fast gapped-read alignment with Bowtie 2. *Nat Methods.*
768 2012; 9(4):357-359.
- 769 98. Di Tommaso P, Chatzou M, Floden EW, Barja PP, Palumbo E, Notredame C. Nextflow
770 enables reproducible computational workflows. *Nat Biotechnol.* 2017; 35(4):316-319.
- 771 99. Harris CR, Millman KJ, van der Walt SJ, Gommers R, Virtanen P, Cournapeau D, et al.
772 Array programming with NumPy. *Nature.* 2020; 585(7825):357-362.

- 773 100. The pandas development team. pandas-dev/pandas: Pandas. 2020.
774 doi:10.5281/zenodo.4067057.
- 775 101. McKinney W. Data Structures for Statistical Computing in Python. Proceedings of the 9th
776 Python in Science Conference. 2010; 445:56-61.
- 777 102. Hoyer S, Hamman J. xarray: N-D labeled Arrays and Datasets in Python. Journal of Open
778 Research Software. 2017; 5(1):10.
- 779 103. Flamary R, Courty N, Gramfort A, Alaya MZ, Boisbunon A, Chambon S, et al. POT: Python
780 Optimal Transport. JMLR. 2021; 22(78):1-8.
- 781 104. Cock PJA, Antao T, Chang JT, Chapman BA, Cox CJ, Dalke A, et al. Biopython: freely
782 available Python tools for computational molecular biology and bioinformatics. Bioinformatics.
783 2009; 25(11):1422-1423.
784

785 **Figure legends**

786 **Fig 1: Enrichment of wildtype peptides.** (A) The x axis indicates each peptide's location along
787 SARS-CoV-2 Spike protein, and each entry on the y axis is an individual sample. All enrichment
788 values over 20 are plotted as 20 to better show the lower range of the data. Above the
789 heatmap, domains of Spike are shown with grey boxes, with the S1/S2 and S2' cleavage sites
790 indicated with arrows. The epitope regions defined in the current study are shown as colored
791 boxes (from left to right: NTD in red, CTD-N' in green, CTD-C' in cyan, pre-FP in pink, FP in black,
792 post-FP in orange, SH-H in purple, and HR2 in blue). (B) Defined epitope regions shown on a
793 structure of one monomer of SARS-CoV-2 Spike in the pre-fusion conformation (PDB 6XR8 [ref
794 95]). The amino acid loci spanned by each epitope are listed. The HR2 epitope (AA 1171-1204)
795 could not be resolved on the structure and is not shown.

796 **Fig 2: Differences in enrichment of wildtype peptides by group.** Wildtype enrichment values
797 were summed for all peptides within each epitope region. Box plots summarize the data by
798 group. (A) compares vaccinated pigtail macaques to vaccinated humans, while (B) compares
799 convalescent rhesus macaques to convalescent humans. Multiple Mann-Whitney U tests were
800 performed, with p values corrected for the number of comparisons in each plot (8) using the
801 Bonferroni-Dunn method. ****, $p \leq 0.0001$; ***, $p \leq 0.001$; **, $p \leq 0.01$; *, $p \leq 0.05$.

802 **Fig 3: Comparison of escape profiles in the CTD-N'.** (A) The top three panels show boxplots
803 depicting the summed differential selection values of all samples in a group at each locus.
804 Negative values represent sites where the binding interaction between antibody and peptide
805 was weakened when peptides were mutated, whereas positive values represent enhanced
806 binding. The bottom panel shows the mean escape similarity score for all pairwise comparisons

807 between samples in each group, calculated at every locus. See S4 Fig for a description of the
808 escape similarity score algorithm. (B) Within- and between-group region-wide escape similarity
809 scores, summarized as boxplots. Each point represents a pairwise comparison between two
810 samples. The contribution of a site's score to the total escape similarity score is weighted based
811 on its relative contribution to the summed differential selection values across the region. P
812 values are not computed due to lack of independence between data points.

813 **Fig 4: Comparison of escape profiles in the fusion peptide (FP).** (A) and (B) Data are shown as
814 described in Fig 3.

815 **Fig 5: Comparison of escape profiles in the stem helix-HR2 region (SH-H).** (A) and (B) Data are
816 shown as described in Fig 3. (C) Logo plots for participant 352 (a convalescent macaque) and
817 M21 (a vaccinated human) showing the effect of specific mutations on antibody binding at each
818 site. The comparison between these samples had an escape similarity score closest to the
819 median value for all pairwise convalescent macaque vs. vaccinated human comparisons and
820 thus can be considered representative of the similarity between these groups. The 352 – M21
821 comparison is shown in red on (B).

822 **Supporting information**

823 **S1 Fig: Enrichment of wildtype peptides varies by group in newly defined epitope regions.** The
824 locus numbers are shown on the x axis, and each individual is represented in a different color.

825 (A) Wildtype enrichment by group from AA 526-685, spanning the CTD-N' and CTD-C' epitopes.

826 (B) Wildtype enrichment by group from AA 777-855, spanning the pre-FP, FP, and post-FP

827 epitopes. (C) Wildtype enrichment by group from AA 1135-1204, spanning the SH-H and HR2

828 epitopes.

829 **S2 Fig: Enrichment of wildtype peptides in baseline macaque samples compared to post-**
830 **vaccination or post-infection samples.** The x axis indicates each peptide's location along SARS-
831 CoV-2 Spike protein, and each entry on the y axis is an individual sample. Sample groups are
832 indicated on the left. The same macaques that contributed baseline samples also contributed
833 post-vaccination or post-infection samples. All enrichment values over 20 are plotted as 20 to
834 better show the lower range of the data. Above the heatmap, domains of Spike are shown with
835 grey boxes, with the S1/S2 and S2' cleavage sites indicated with arrows. The epitope regions
836 defined in the current study are shown as colored boxes (from left to right: NTD in red, CTD-N'
837 in green, CTD-C' in cyan, pre-FP in pink, FP in black, post-FP in orange, SH-H in purple, and HR2
838 in blue).

839 **S3 Fig: Differences in enrichment of wildtype peptides by macaque subgroups.** Wildtype
840 enrichment values were summed for all peptides within each region of Spike that showed
841 enrichment. Each point represents an individual macaque. No significant differences were
842 found by Kruskal-Wallis test at a threshold of $p=0.05$. LION: Lipid InOrganic Nanoparticle; NLC:
843 Nanostructured Lipid Carrier.

844 **S4 Fig: Use of optimal transport to quantify similarity between amino acid escape profiles.** (A)
845 Profile 1 and 2 show example logo plots for two samples across the same region. Negative
846 scaled differential selection values represent mutations that reduce antibody binding. Amino
847 acids of the same color indicate similar chemistry (e.g., green = polar). (B) At each location (in
848 this example, the boxed site in panel A), the profiles are represented as binned distributions
849 where each bin corresponds to the contribution to escape for an amino acid substitution. (C)
850 The optimal transport solution to transform one profile to the other is computed, where the

851 cost to "exchange" an amino acid contribution in Profile 1 to an amino acid contribution in
852 Profile 2 is derived from the BLOSUM62 matrix. For the purposes of the schematic, the number
853 of dollar signs associated with each line denotes the relative cost of each move (i.e., more
854 dollar signs = more costly = moving between amino acids that are less similar). (D) To quantify
855 similarity between profiles, an escape similarity score is calculated as the inverse of the total
856 cost to perform the transformation. For more details, see
857 <https://matsengrp.github.io/phipperry/esc-prof.html>. Created with BioRender.com.

858 **S5 Fig. Logo plots for all vaccinated macaques, vaccinated humans, and convalescent**
859 **macaques in the CTD-N' epitope region.**

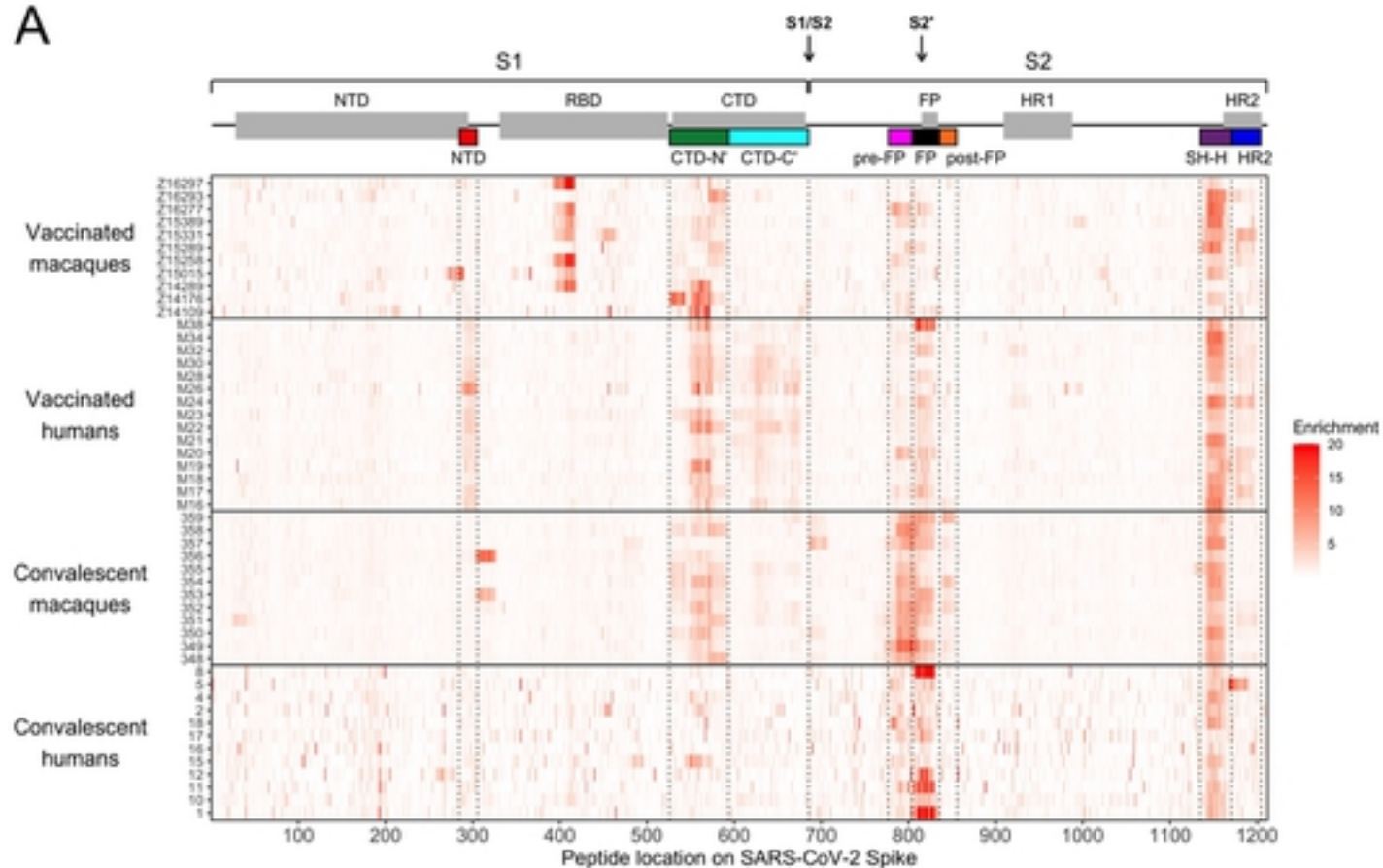
860 **S6 Fig. Logo plots for all vaccinated humans, convalescent macaques, and convalescent**
861 **humans in the FP epitope region.**

862 **S7 Fig. Logo plots for all vaccinated macaques, vaccinated humans, convalescent macaques,**
863 **and convalescent humans in the SH-H epitope region.**

864 **S8 Fig. Logo plots for all convalescent macaques in the pre-FP and post-FP epitope regions.**

865 **S9 Fig: Differences in enrichment of wildtype peptides in vaccinated humans and**
866 **convalescent macaques.** As in Fig 2, wildtype enrichment values were summed for all peptides
867 within each epitope region of Spike. Multiple Mann-Whitney U tests were performed, with p
868 values corrected for the number of comparisons (8) using the Bonferroni-Dunn method. ****, p
869 ≤ 0.0001 ; ***, $p \leq 0.001$; **, $p \leq 0.01$; *, $p \leq 0.05$.

A



B

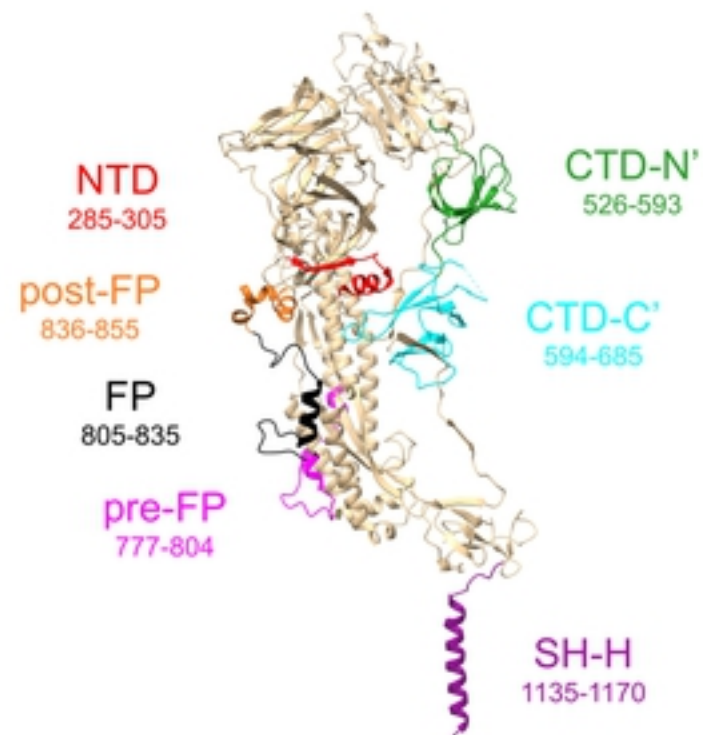
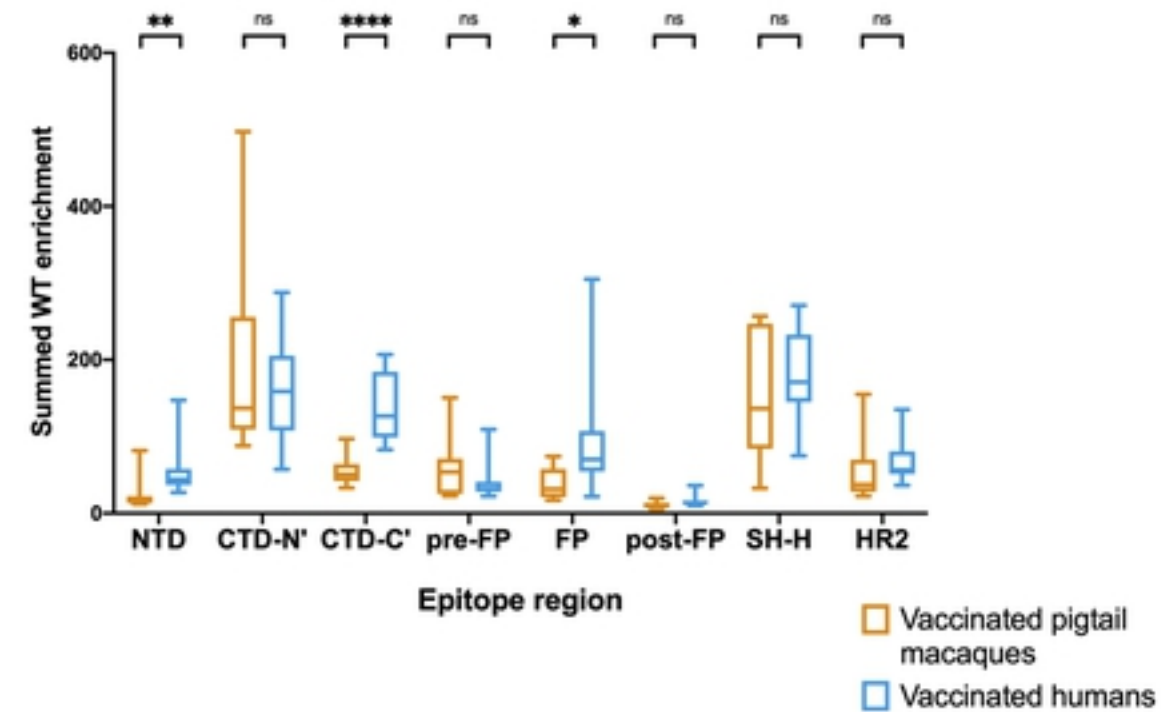


Figure 1

A



B

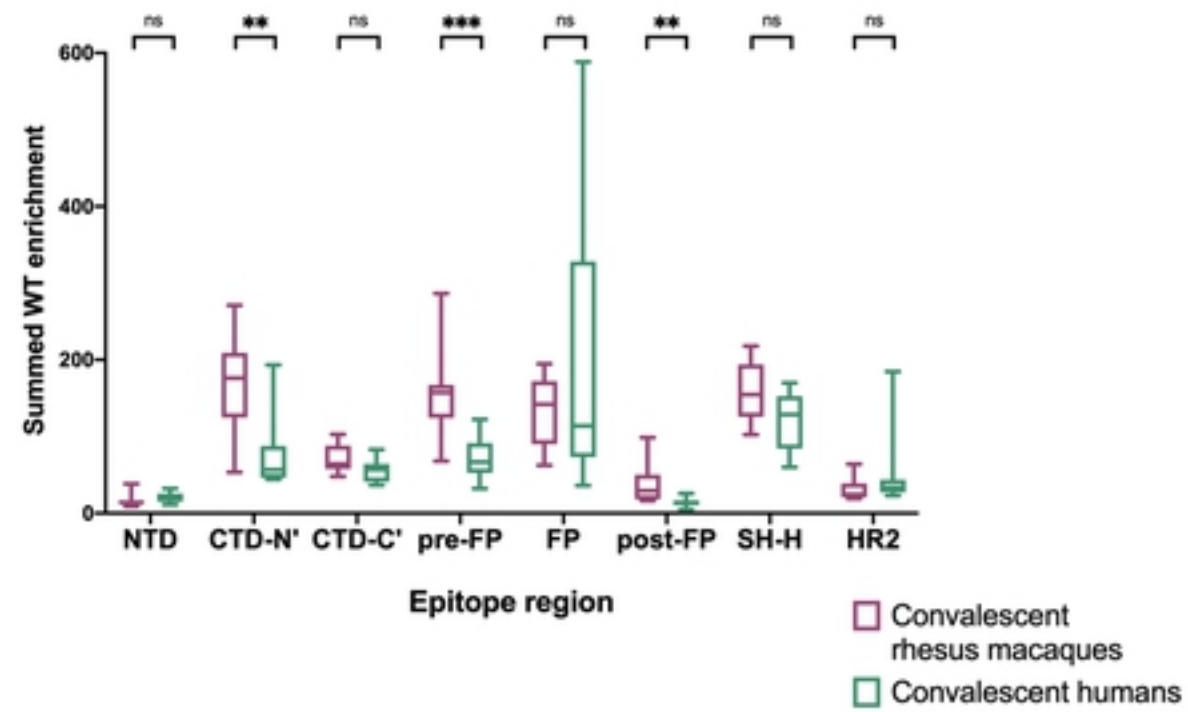


Figure 2

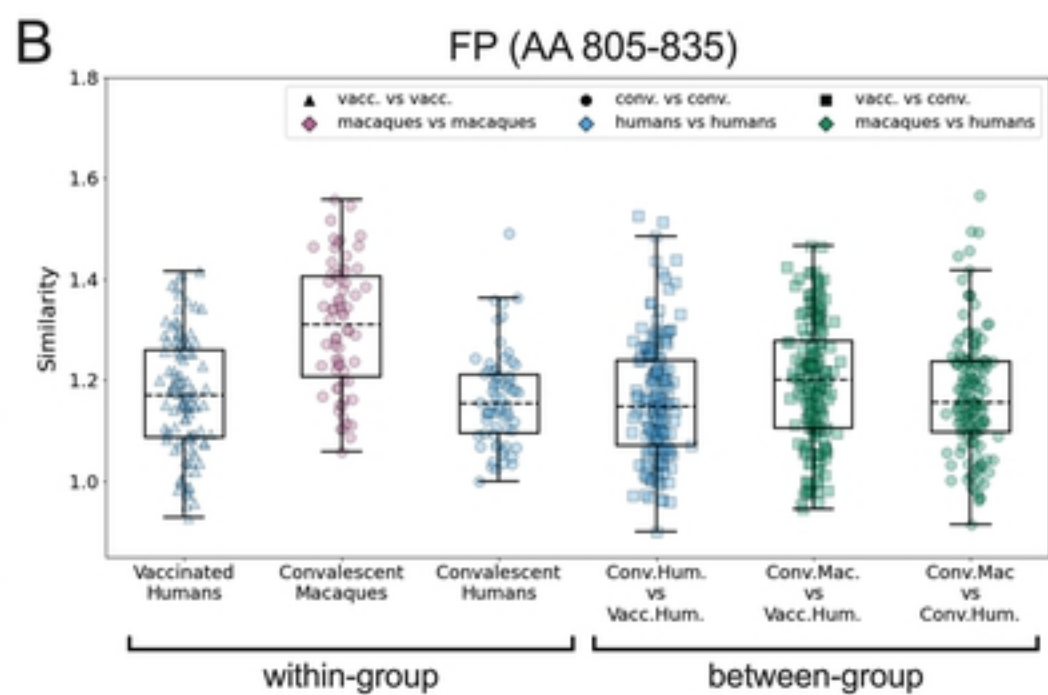
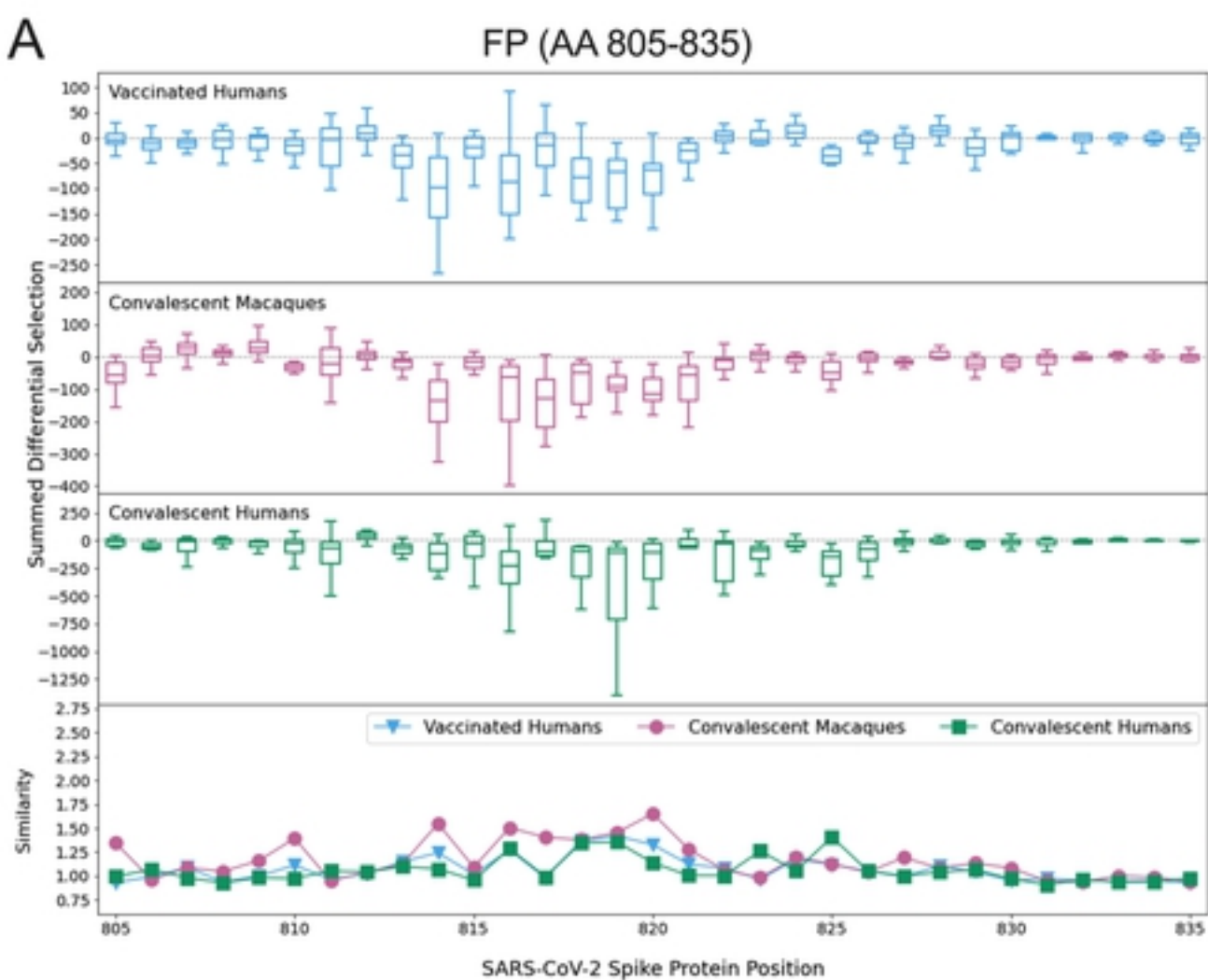


Figure 4

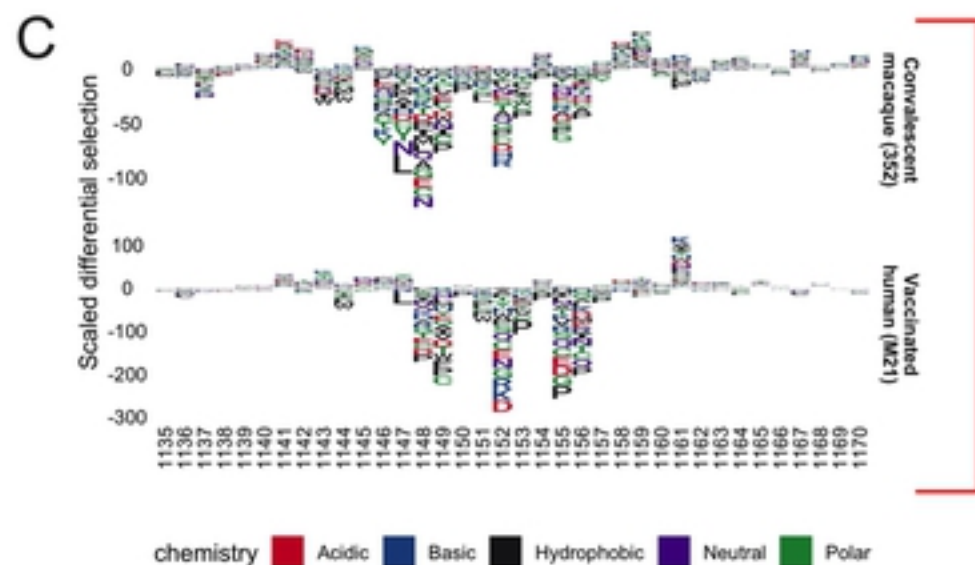
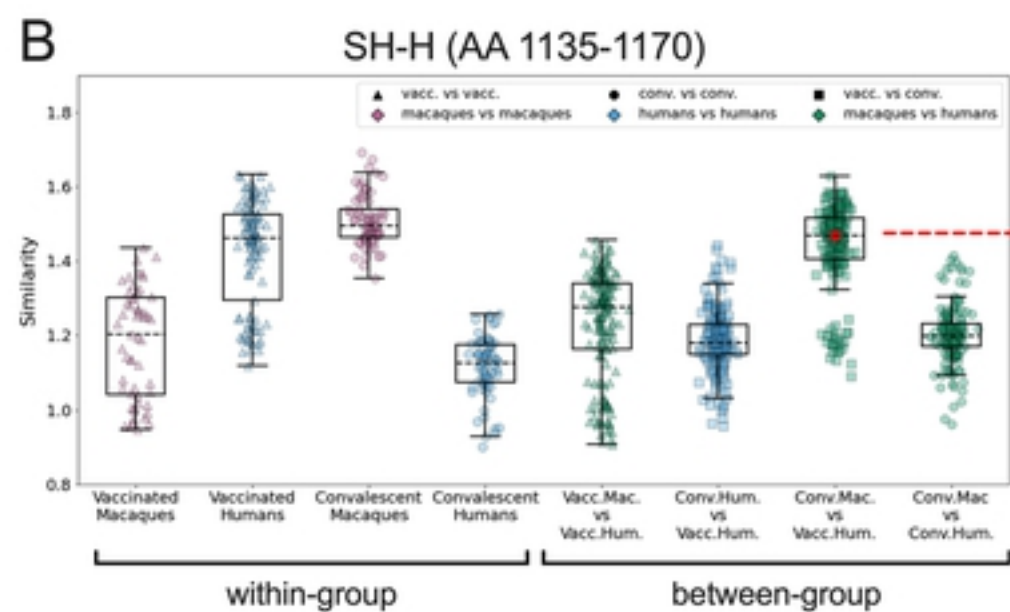
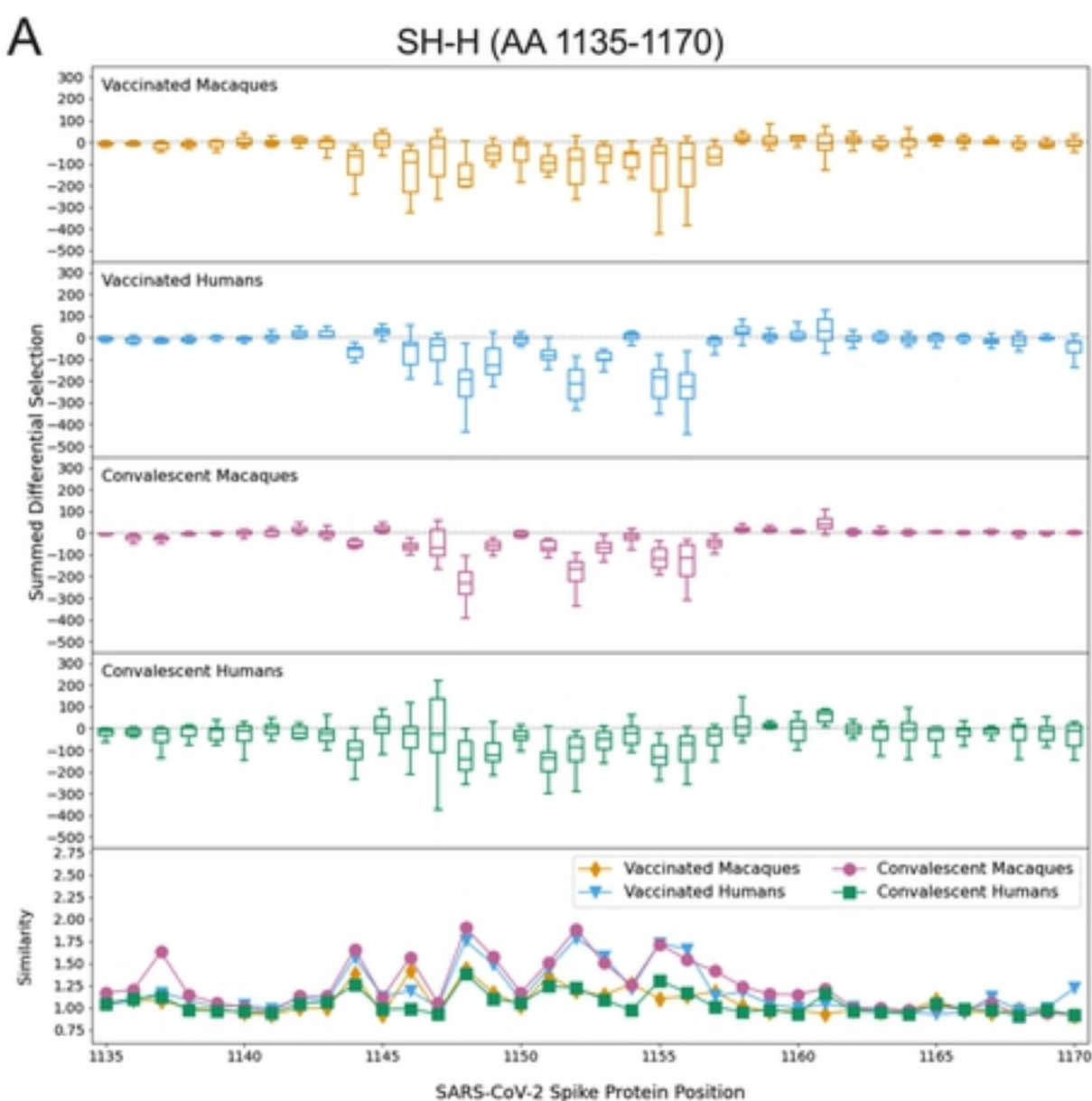


Figure 5